J. Fluid Mech. (1971), *vol.* 49, *part* 4, *pp.* 803–816
Printed in Great Britain

Aerodynamic excitation of the harmonium reed

By ARTHUR O. ST HILAIRE,† THEODORE A. WILSON AND GORDON S. BEAVERS

Department of Aerospace Engineering and Mechanics,
University of Minnesota, Minneapolis, Minnesota

(Received 25 February 1971)

An investigation of the mechanism responsible for the self-excited oscillations of a harmonium reed is presented. Experiments show that the amplitude of vibration of the reed grows exponentially, and measurements of the growth rate as a function of the flow past the reed are reported. Flow visualization studies lead to the conclusion that jet or wake instability is not important in exciting the reed vibration. An analysis of the flow around the reed as an unsteady potential flow results in the evaluation of the aerodynamic forces exciting the reed. The analysis shows that the pressure which excites the reed motion is of the order of $\rho U_0 \dot{a}$, where U_0 is the flow velocity and $\dot{a}$ is the reed velocity.

1. Introduction

The study of acoustics from a fluid mechanics point of view has received considerable attention in recent years, with particular emphasis directed towards the noise generated by jets, wakes and boundary layers. A group of sound sources which appear to have been studied much less thoroughly are those found in the wind instruments and whistles. This group includes an interesting variety of sound sources, all of which have been developed empirically to satisfy the criteria that they be efficient producers of sounds of a definite, controllable, and audible pitch, and that they be operable under flow conditions which can be produced by the human lungs. The aerodynamics of many of these sources is still not well-understood, whereas the acoustic properties of the resonators associated with the various sources have been studied rather extensively in many cases. The mechanics of these familiar devices, however, would seem to have some intrinsic interest, and may possibly be of technological interest in certain applications concerned with preventing or controlling sound production and vibration.

Experimental investigations of the unsteady flow associated with sound production have raised several interesting questions in fluid mechanics, while providing enough information to classify some of the sources according to their basic mechanism. It would appear that these sources can be divided into four groups characterized by the nature of the fluid-mechanical instabilities which are responsible for the self-excited oscillations of the flow.

The first class of sound sources, and the one that has received the most attention, consists of the edge tones. These sources depend on the instability of a

† Present address: Mechanical Engineering Department, Tufts University.

well-developed plane jet to the formation of an alternating vortex street, and the subsequent interaction of the vortices with a solid boundary upon which the jet impinges. They include the edge tone itself (Brown 1937; Curle 1953), and the edge tone coupled to a resonator, as in the organ pipe (Cremer & Ising 1967) and in the flute (Coltman 1968).

A second class of sound sources consists of the hole tones. The mechanism which is common to the devices belonging to this class is the instability of an undeveloped jet to the formation of vortex rings and the interaction of the rings with a stationary boundary in the flow. Typical members of this class are the Pfeifentöne (Anderson 1955), the Rayleigh bird-call (Chanaud & Powell 1965), and human whistling (Wilson *et al.* 1971).

There are other wind instruments which depend, for their operation, on the presence of a vibrating boundary in the flow. These instruments can be divided into two groups which comprise the remaining two of the proposed four basic classes. One of these groups consists of the reed instruments. For this group the geometry of the flow is such that the flow separates from the reed at a sharp edge and the streamlines along the reed surface turn through an angle greater than 90° in forming the free jet. It is shown in this paper that the pressure forces developed in the unsteady potential flow past the reed excite the reed vibration.

There are sound sources associated with other wind instruments which involve a vibrating boundary in the flow, but which have geometries which do not meet the requirements for the mechanism responsible for the excitation of the reed vibrations. The vibrating lips in the playing of brass instruments, the vocal cords and the vibrating membrane of birds are apparently members of a fourth group having an excitation mechanism differing from that for the reed instruments. The fundamental mechanism for this group may depend on an unsteady boundary-layer effect.

This paper is concerned primarily with one member of the reed-instrument class of sound sources, namely the type of metal reed used in the harmonica and the harmonium (reed organ). Flow visualization studies are described which indicate that jet instability is not important in exciting the reed vibrations. The paper then describes an analysis of the potential flow through the slit bounded by the reed and the supporting structure. The aerodynamic forces which excite the vibration of the reed are calculated and comparisons with experiment are presented to substantiate the analysis.

2. Geometry and operation of the harmonium reed

The geometries of the harmonium reed and the harmonica reed are similar, and are shown in figure 1. The reed is essentially a thin metal plate which is riveted at one end to a support plate so that in the undisturbed position the reed is situated just above the plane of the support. In the harmonium, the support plate forms an integral part of the shallot, and throughout this paper the term shallot will be used when referring to this support plate. There is a rectangular opening in the shallot immediately beneath the reed, the size of the opening being slightly larger than the reed. This configuration allows the reed to vibrate as a canti-

levered beam. The geometry of a typical reed is such that the size a of the gap between the reed and the shallot plane is small compared with the reed width h which, in turn, is small compared with the length l of the reed. Furthermore, all reed dimensions are small compared with the wavelength of the sound being produced by the reed. It follows that it is reasonable to expect that the flow within distances less than l away from the reed is nearly two dimensional and that the fluid is nearly incompressible in the flow near the reed.

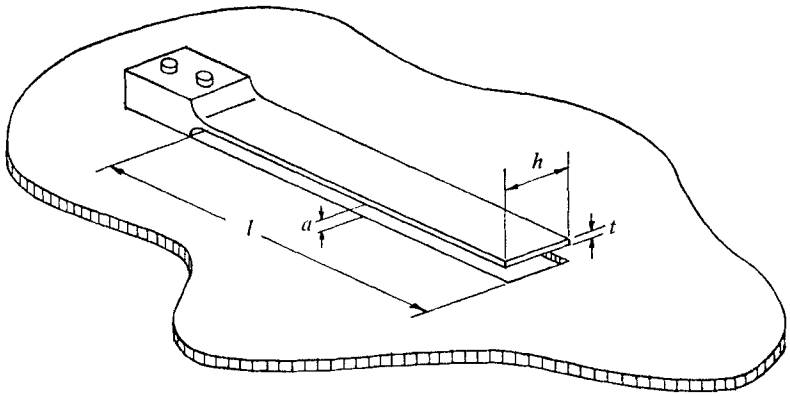

FIGURE 1. Schematic of the harmonium reed and shallot plate.

Reed	f_0(Hz)	t(cm)	h(cm)	l(cm)	a(cm)
A	165	0·022	0·58	3·80	0·035
B	225	0·030	0·46	4·20	0·020

TABLE 1. Reed characteristics

A self-excited oscillation of the reed occurs when the pressure on the top of the shallot is raised and a sufficient flow through the gaps between the reed and the shallot is produced. From the point of view of considering the aerodynamic forces on the reed as drag forces, it is somewhat surprising that the forces will excite the reed vibration. In order for the flow to put energy into the reed motion, the drag must be reduced when the reed is moving upward, against the flow, and the drag must increase when the reed is moving downward, in the direction of the flow.

In order to study the growth of the reed vibration in the laboratory, two reeds were removed from a reed organ and each was attached to an appropriate shallot. The dimensions of the two reed assemblies are given in table 1, which also includes the natural frequency f_0 of each reed.

The shallot plate formed one wall of a plenum chamber. The flow rate through the slot in the shallot was measured by means of a calibrated orifice set in the air supply line to the plenum chamber. The amplitude of the bending of the reed was determined by the use of a strain gauge attached to the upstream surface of the reed close to the point of support. Measurements of the decay or growth of the reed vibration were made over a range of flow rates. This was accomplished by

fixing the flow rate and then releasing the reed, either from a displaced position if the flow was too low to excite the vibrations, or from the equilibrium position if the flow was high enough to excite the vibrations. Typical oscillograms showing the time history of the strain gauge output are shown in figure 2 (plate 1).

The experiments revealed that the vibration amplitude decays exponentially for small enough amplitudes, and also that the growth under self-excitation is exponential up to an amplitude of about 40 % of the limiting amplitude. Hence, for small amplitudes, the amplitude is proportional to $e^{\epsilon t}$. The values of the

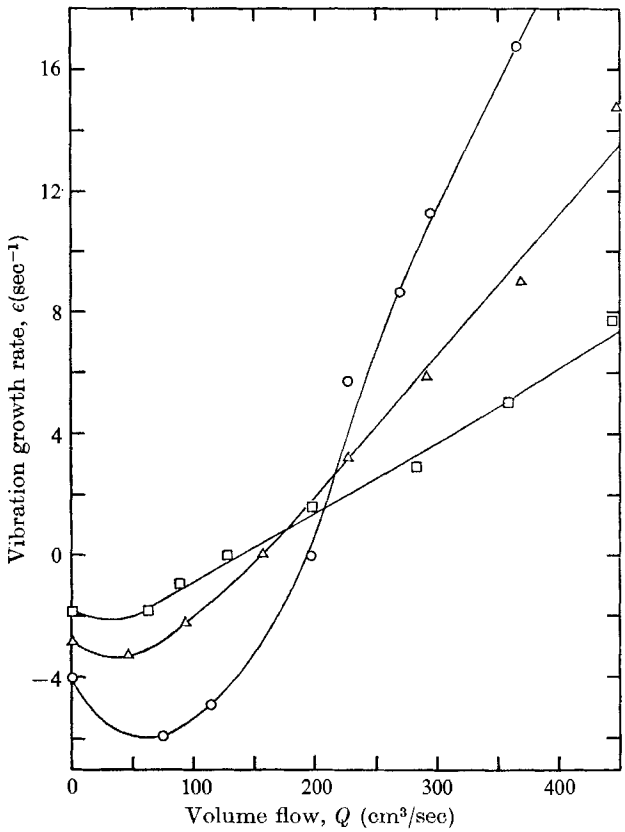

FIGURE 3. Vibration growth rate as a function of volume flow rate for reed A. f (Hz): ○, 165; △, 137; □, 120.

quantity ϵ were found by inspection of the oscillograms, and are plotted as a function of the flow rate Q in figures 3 and 4. Also shown on these figures are results obtained when the reeds were modified by the addition of small masses to the reed tips. These masses were used to reduce the vibration frequency of the reed without changing the reed geometry. The amplitude decay at zero flow is assumed to be due to material damping. Figures 3 and 4 show that the aerodynamic forces add to the damping for small flows, but for higher flows the vibration becomes self-excited and at high values of the flow rate the growth rate increases nearly linearly with Q.

3. Flow visualization experiments

Flow visualization studies were carried out to determine whether a jet instability could be the mechanism driving the reed vibration. Preliminary studies were made using the harmonium reeds and the flow system described earlier. Smoke was added to the air in the plenum chamber supplying the flow to the reed, and stroboscopic lighting was used to view the flow field near the reed. The

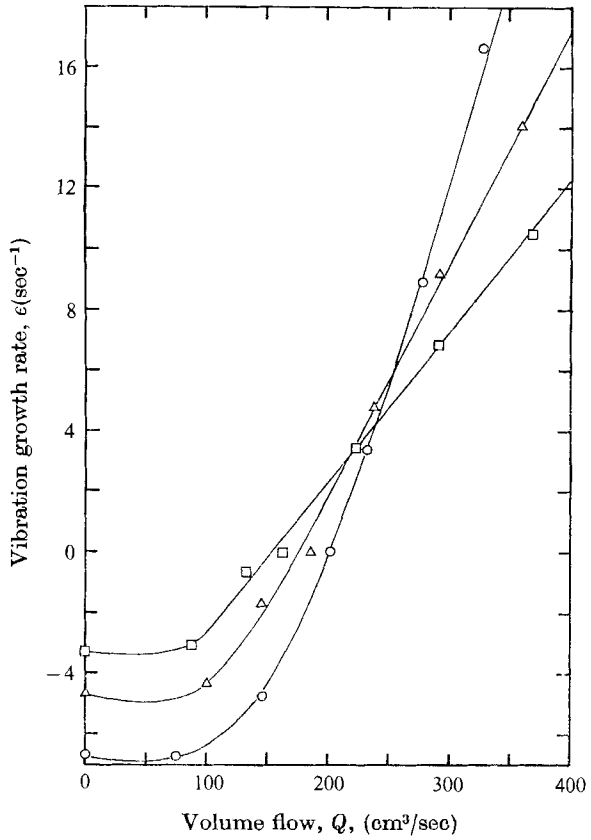

FIGURE 4. Vibration growth rate as a function of volume flow rate for reed B. f(Hz): ○, 225; △, 190; □, 161.

small size of the reed, however, resulted in some difficulty in observing the flow pattern, with a consequent uncertainty concerning the presence or absence of jet instability. Nevertheless, these experiments did reveal that the flow in the vicinity of the reed was two-dimensional.

Since no definitive conclusions concerning jet instability could be drawn from the smoke experiments, model flow visualization experiments were run in a water tunnel. This facility, which is capable of providing uniform accurately-known flows, has been described in detail elsewhere (Beavers & Wilson 1970). Visualization of the flow field was accomplished by the injection, via hypodermic tubes,

of four neutrally-bouyant dye streams into the flow on the upstream walls of both the model reed and the shallot plate. The model reeds were positioned in the tunnel test-section such that experiments could be performed with the reeds both stationary and oscillated by an external driver.

Typical flow patterns are shown in figures 5 and 6 (plate 2). It can be seen that the flow separates at the gaps and the two free jets intersect and combine downstream of the reed. The angle between the direction of each jet and the plane of the reed agrees well with the prediction of the potential flow analysis of the formation of a free jet in this geometry (Birkhoff & Zarantonello 1957). Figure 5 shows flow patterns for the reed held stationary at a large distance from the plane of the shallot ($h/a = 4{\cdot}37$). At low flow rates (figure 5 (*a*)) the vortex formation in the vortex sheets bounding the jets was always observed to be symmetric, similar to that observed in single jets (Beavers & Wilson 1970). On the other hand, at higher flow rates (figure 5 (*b*)) the vortex formation appeared to become alternating. Figure 6 compares flow patterns with the reed held stationary with corresponding patterns at the same flow rates with the reed oscillating with a very small amplitude about a mean position such that $h/a \approx 15$. The flow rates for these experiments were adjusted to correspond to flows near the extremes of the operating range in the real situation. In all comparisons no major differences in the flow patterns could be discerned.

Although vortex streets are formed in the jet downstream of the reed, the Strouhal number for the vortex formation was always observed to be more than a factor of 10 higher than the Strouhal number based on the reed frequency. Even when the model reed was oscillated at a frequency suitably scaled for the experiments, no clear periodic jet instability having the frequency of the reed vibration was excited in the vicinity of the reed. It was concluded, therefore, that, unlike the mechanism for exciting the edge tones, hole tones and Aeolian tones, the jet or wake instability is not important in exciting the reed vibrations. This conclusion is consistent with the fact that the Strouhal number of the reed vibration, fa/U_0, is less than 0·01, a value which is less than the reported Strouhal numbers associated with jet and wake instabilities. Furthermore, it is consistent with the observation that the vibration amplitude of the reed grows exponentially, which implies that the force which excites the vibration has an amplitude which is proportional to the amplitude of the vibration. This would not be expected to be the case if the force arose from a jet instability which is only triggered or regulated by the reed vibration.

4. Analysis of the flow

The unsteady potential flow for the reed geometry is now analyzed and the pressure forces which add energy to the reed motion are evaluated. An approximate analysis of the flow is made by dividing the flow into five regions, as shown in figure 7, in which different approximate descriptions of the flow are appropriate. In the actual reed configuration the reed is situated a small distance a above the shallot plane in the early stages of the amplitude growth, thus creating two gaps each of which has an area given approximately by al. In this analysis the flow past

the reed is approximated by assuming that the reed lies in the shallot plane, with a gap of width a on either side of the reed.

The first flow region to be described is the region upstream of the gaps and near the reed where the flow is very nearly two-dimensional. This is designated as region I in figure 7. The flow in this region is approximately that due to two line

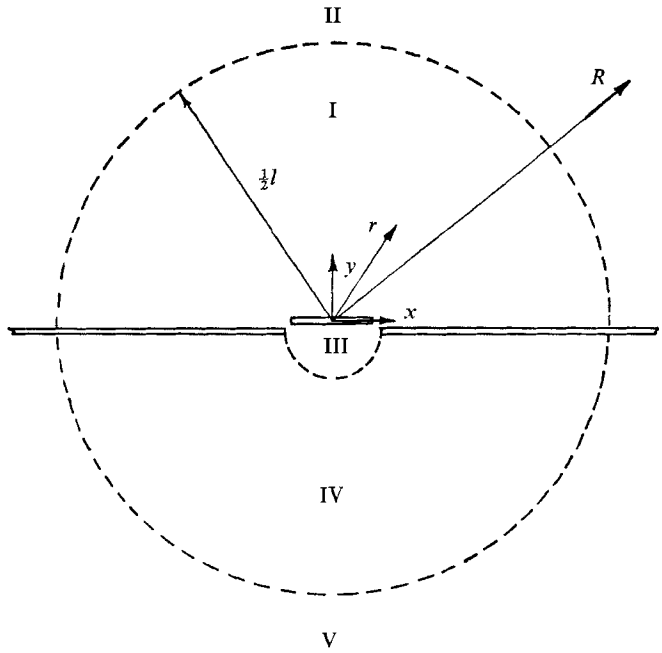

FIGURE 7. The assumed flow regions surrounding the reed.

sinks located at $x = \pm x_0$, $y = 0$, where $x_0 = \frac{1}{2}(h+a)$, together with a uniform source distribution over the entire reed surface. The source distribution is required to match the boundary conditions imposed on the flow by the reed motion. The potential in region I is then given by

$$\begin{aligned}\phi_{\mathrm{I}} = &-(Q/4\pi l)\ln[(x^2-y^2-x_0^2)^2+4x^2y^2]\\ &-(\dot{a}l/2\pi l)\Big\{(x-\tfrac{1}{2}h)\ln[(x-\tfrac{1}{2}h)^2+y^2]\\ &-(x+\tfrac{1}{2}h)\ln[(x+\tfrac{1}{2}h)^2+y^2]\\ &+2y\Big[\tan^{-1}\Big(\frac{x-\frac{1}{2}h}{y}\Big)-\tan^{-1}\Big(\frac{x+\frac{1}{2}h}{y}\Big)\Big]\Big\},\end{aligned} \tag{1}$$

where Q is the total volume flow through the two gaps, each of constant length l, and $\dot{a}l$ is the rate at which each gap area is changing. When the cylindrical radial co-ordinate r is large compared with the reed width h, the expression for ϕ_{I} can be approximated by

$$\phi_{\mathrm{I}} = -\Big(\frac{Q-hl\dot{a}}{\pi l}\Big)\ln r. \tag{2}$$

At distances larger than the reed length l, the flow is three dimensional and a second region (II) is introduced in which the flow is assumed to be that due to a three-dimensional sink situated at the reed centre. The potential in region II is thus given by the expression

$$\phi_{\mathrm{II}} = \frac{Q - hl\dot{a}}{2\pi R}, \tag{3}$$

where R is the spherical radial co-ordinate.

Attention is now turned to the flow field downstream of the reed. Here the flow is divided into three distinct regions in which different approximations are introduced. Experiments have shown that the flow separates from the reed and the shallot at the gaps and forms two free jets. The downstream side of the reed is covered by the 'dead water' region bounded by the jets (figures 5 and 6). Furthermore, the flow visualization experiments indicated that this fluid moves with the reed. A simple approximation, therefore, is to assume that there exists a region III just behind the reed and extending to approximately $r = \frac{1}{2}h$ in which the pressure is uniform. Further away from the reed, the unsteady flow into the region downstream of the shallot produces a flow which is approximately two dimensional. This region is indicated by region IV in figure 7. Finally, at large distances from the reed, there exists a three-dimensional source flow (region V) corresponding to the three-dimensional sink flow on the upstream side of the shallot. The potentials in regions IV and V can be written in forms analogous to the potentials in regions I and II respectively. However, there would be very little pressure recovery in the flow downstream of the reed if the flow were steady. Thus only the unsteady part of the volume flow through the gaps, δQ, is included in the potentials ϕ_{IV} and ϕ_{V} which are to be used to compute the pressure field downstream of the reed. The appropriate forms of the potentials are therefore

$$\phi_{\mathrm{IV}} = \left(\frac{\delta Q - hl\dot{a}}{\pi l}\right) \ln r \tag{4}$$

and

$$\phi_{\mathrm{V}} = -\left(\frac{\delta Q - hl\dot{a}}{2\pi R}\right). \tag{5}$$

The potentials expressed above are now used to compute the pressure field. This is achieved by equating the pressures on the two sides of each of the boundaries separating the various flow regions. The overlapping of the boundaries separating regions I and II, and IV and V, are neglected within the spirit of the assumptions already made in the analysis. There is a logarithmic singularity in the pressure at the edge of the reed on the upstream side, and thus the connection between regions I and III is best made at the edge of the shallot. This is done by setting the pressure in region III equal to the pressure in region I at the point $x = \frac{1}{2}h + a$, $y = 0$. The pressure difference between the upstream and downstream reservoir pressures is then given in terms of the flow variables, and to lowest order in a/h, by the expression

$$\frac{\Delta p_0}{\rho} = \frac{1}{2}\frac{Q^2}{\pi^2 l^2 a^2} + \frac{\dot{Q}}{\pi l}\left[2 + \ln\left(\frac{l^2}{h(2ha)^{\frac{1}{2}}}\right)\right] - \frac{Q\dot{a}}{\pi^2 la}\ln\left(\frac{h}{a}\right) - \frac{h\ddot{a}}{\pi}\left[2 + \ln\left(\frac{l^2}{2h^2}\right)\right]. \tag{6}$$

The flow rate and gap size are now assumed to be given by

$$\left.\begin{aligned} Q &= Q_0 + Q_1 e^{iwt}, \\ a &= a_0 + a_1 e^{iwt}. \end{aligned}\right\} \tag{7}$$

When equations (7) are substituted into (6) and only linear terms in the perturbation quantities are retained, the relation between Q_1 and a_1 is obtained in the form

$$\frac{Q_1}{Q_0} = \frac{\left[1 - \frac{\pi w^2 h l^2 a_0^3}{Q_0^2}\left[2 + \ln\left(\frac{l^2}{2h^2}\right)\right] + i\frac{wla_0^2}{Q_0}\ln\left(\frac{h}{a_0}\right)\right]\frac{a_1}{a_0}}{1 + i\frac{\pi wla_0^2}{Q_0}\left[2 + \ln\left(\frac{l^2}{h(2ha_0)^{\frac{1}{2}}}\right)\right]}. \tag{8}$$

It can be seen from equation (8) that if the frequency of the gap oscillation is small, the fractional change in the volume flow is the same as the fractional change in the gap size. On the other hand, at higher frequencies, the flow perturbation is reduced and lags behind the gap perturbation on account of the inertia of the fluid.

The objective of the analysis is to calculate the component of the unsteady force which is in phase with the reed velocity. This unsteady force component is derived from the pressure difference across the reed, which can now be calculated. The pressure over the downstream side of the reed is uniform and is equal to the pressure at the edge of the shallot on the upstream side. Thus the pressure difference Δp between the top and the bottom of the reed is given approximately by the quantity $[p(x, y = 0) - p(x = a + \frac{1}{2}h, y = 0)]$ evaluated in region I. This yields the following expression for Δp

$$\begin{aligned} \frac{\Delta p}{\rho} = \frac{\Delta p_0}{\rho} &- \frac{1}{2}\frac{Q^2}{\pi^2 l^2}\frac{x^2}{(x_0^2 - x^2)^2} - \frac{\dot{Q}}{2\pi l}\left[4 + \ln\left(\frac{l^4}{4h^2(x_0^2 - x^2)}\right)\right] \\ &- \frac{Q\dot{a}}{\pi^2 l}\left[\frac{x}{x_0^2 - x^2}\ln\left(\frac{\frac{1}{2}h + x}{\frac{1}{2}h - x}\right)\right] \\ &+ \frac{\ddot{a}}{\pi}\left[2h + h\ln\left(\frac{l^2}{2h}\right) - x\ln\left(\frac{\frac{1}{2}h + x}{\frac{1}{2}h - x}\right) - \tfrac{1}{2}h\ln\left(\tfrac{1}{4}h^2 - x^2\right)\right]. \end{aligned} \tag{9}$$

The component of the pressure difference which is in phase with the velocity is then obtained by substituting equations (7) into (9), using (8) to replace Q_1 by a_1. Upon collecting terms which are linear in a_1, of lowest order in a_0/h and in phase with $\dot{a}$, an expression for the in-phase pressure component δp is obtained, which is

$$\frac{\delta p}{\rho} = -\frac{Q_0}{2\pi l}\frac{\left[4 + \ln\left(\frac{l^4}{4h^2(x_0^2 - x^2)}\right)\right]\left[1 - \frac{\pi w^2 h l^2 a_0^3}{Q_0^2}\left(2 + \ln\frac{l^2}{2h^2}\right)\right]\left(\frac{\dot{a}}{a_0}\right)}{\left[1 + \frac{\pi^2 w^2 l^2 a_0^4}{Q_0^2}\left(2 + \ln\left(\frac{l^2}{h(2ha_0)^{\frac{1}{2}}}\right)\right)^2\right]}. \tag{10}$$

Finally, the average force per unit area, $\overline{\delta p}$, which excites the reed motion is obtained by integrating this pressure difference over the reed surface

$$\overline{\delta p} = \frac{1}{h}\int_{-\frac{1}{2}h}^{\frac{1}{2}h} (-\delta p)\, dx,$$

where a change of sign is introduced so that positive $\overline{\delta p}$ is in the direction of increasing y (figure 7). The integration of equation (10) yields

$$\frac{\overline{\delta p}}{\left(\frac{\rho Q_0 \dot{a}}{2la_0}\right)} = \frac{\frac{2}{\pi}\left[3+\ln\left(\frac{l^2}{2h^2}\right)\right]\left[q^2-\frac{h}{\pi a_0}\left(2+\ln\left(\frac{l^2}{2h^2}\right)\right)\right]}{q^2+\left[2+\ln\left(\frac{l^2}{h(2ha_0)^{\frac{1}{2}}}\right)\right]^2}, \tag{11}$$

where

$$q = Q_0/\pi w l a_0^2. \tag{12}$$

Inspection of equation (11) shows that the aerodynamic force will add to the damping for small values of q, whereas it will add energy to the vibration for large values of q. The magnitude of the force is of the order of $\rho U_0 \dot{a}$ per unit area, where U_0 is an average jet speed given by $Q_0/2la_0$.

5. Comparison of analytical and experimental results

The experimental data can be compared with the analytical results most conveniently by computing an effective value of $\overline{\delta p}$ from the experimental data and comparing this with the value given by equation (11). The experimental value of $\overline{\delta p}$ is obtained by computing the force which is required to produce the observed rate of change of the reed energy E. This is accomplished by noting that the work done by the pressure forces is equal to the observed energy change minus the energy change due to material dissipation. This latter quantity is assumed to be given by the damping at zero flow, so that the equation giving the pressure force is

$$\frac{1}{E}\int_S (-\delta p)\dot{a}\,dS = \frac{\dot{E}}{E} - \left(\frac{\dot{E}}{E}\right)_{Q=0}, \tag{13}$$

where the integral is taken over the surface S of the reed. If δp is proportional to $\dot{a}$, then $\delta p/\dot{a}$ is constant over the reed surface and can be taken out of the integral. Furthermore, for a uniform reed the quantity

$$E\Big/\int_S a^2\,dS$$

is just the mass per unit area of the reed; and since the mode shape is nearly the same for the reeds loaded with a mass at the tip as for the uniform reed, this quantity can be approximated by the relationship

$$E\Big/\int_S \dot{a}^2\,dS = \rho_B t\left(\frac{f_0}{f}\right)^2, \tag{14}$$

which can be used for both loaded and unloaded reeds. In (14), ρ_B is the density of the reed, t is the reed thickness, f_0 is the frequency of vibration of the unloaded reed, and f is the frequency of the reed, either loaded or unloaded. Finally, since the reed energy is proportional to the square of the vibration amplitude, the vibration growth rate ϵ can be written in terms of the energy change by the expression

$$\epsilon = \dot{E}/2E.$$

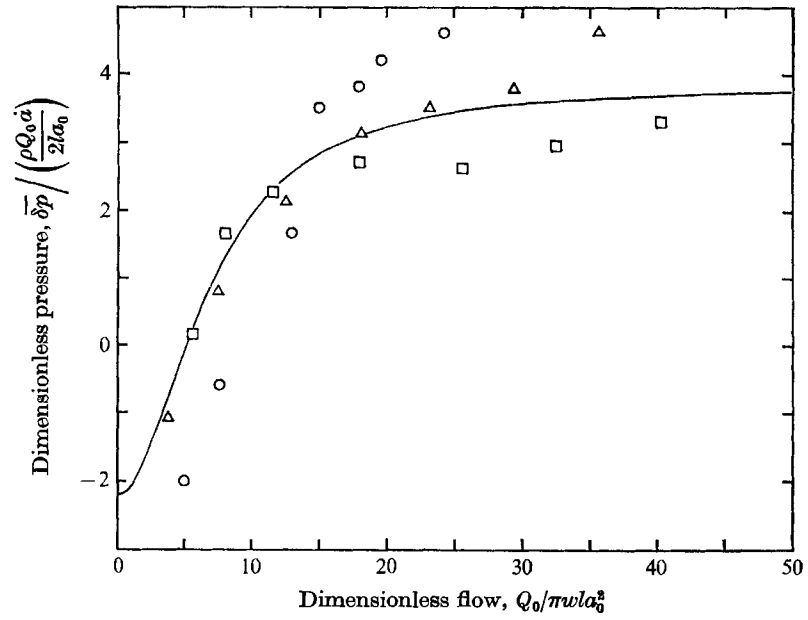

FIGURE 8. Dimensionless pressure force as a function of dimensionless volume flow rate for reed *A*. f(Hz): ○, 165; △, 137; □, 120; —, equation (11).

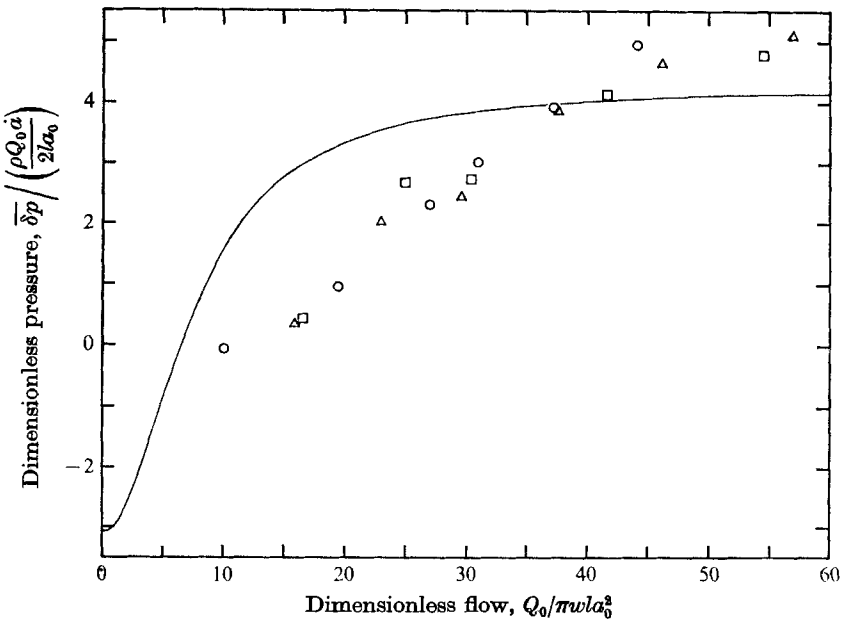

FIGURE 9. Dimensionless pressure force as a function of dimensionless volume flow rate for reed *B*. f(Hz): ○, 225; △, 190; □, 161; —, equation (11).

It follows that a dimensionless experimental value of $\overline{\delta p}$ can be computed from the data by means of the expression

$$\frac{\overline{\delta p}}{(\rho Q_0 \dot{a}/2la_0)} = \frac{\rho_B}{\rho}\frac{t}{a_0}\frac{2(\epsilon - \epsilon_{Q=0})}{\pi^2 fq}\left(\frac{f_0}{f}\right)^2. \tag{15}$$

The experimental and analytical values of $\overline{\delta p}$ for the two reeds are shown in figures 8 and 9. It can be seen that the non-dimensionalizations of Q_0 and $\overline{\delta p}$ which were obtained from the analysis are successful in bringing the experimental data for different frequencies close to a common curve, and that the order of magnitude of the experimentally determined force agrees with the results predicted by the analysis. The qualitative features of the shapes of the experimental and analytical curves are similar, but for reed B (figure 9) the value of q at which the aerodynamic force changes sign is observed to be higher than the value predicted by the analysis. Several factors may contribute to this discrepancy. The gap size for this reed is very small, so that a small difference between the width of the shallot slot and the width of the reed would make the effective gap size somewhat larger, with a corresponding reduction in the experimental values of q. In addition, this reed has a slight taper from the base to the tip, so that the effective length is therefore somewhat less than the actual total length.

In conclusion, figures 8 and 9 indicate that the agreement between experiment and analysis is good considering the non-uniformity of the reeds and the approximations involved in the analysis.

6. Discussion

The mechanism responsible for the excitation of the reed vibration can be described qualitatively by reference to the analytical results derived earlier. When the reed is moving upwards, the gap size is increasing and thus, from (8), the flow is increasing. It follows by inspection of (9) that the pressure above the reed rises towards the upstream reservoir pressure more slowly with distance from the edge of the reed than it would if the flow were steady. It may be deduced from (10) that the pressure on the upper surface of the reed is reduced when the gap size is increasing and the flow is accelerating. This occurs because most of the fluid inertia is contained in the fluid far from the gaps. Conversely, when the gap size is decreasing, and the flow therefore is decelerating, the pressure on the upper surface of the reed is slightly higher than it would be for steady flow. Parenthetically, it must be pointed out that the effect is reversed at low volume flow rates, when the volume displacement of fluid resulting from the reed motion becomes the dominant factor. For example, as the gap size increases, the volume displacement more than offsets the requirements for an increasing flow through the gaps, so that the fluid far from the gaps must be decelerating. However, at higher values of the upstream reservoir pressure, and therefore higher flows, the rate of volume displacement due to the reed motion is negligible compared with the change in the flow resulting from the variation in gap size.

There are certain requirements which must be met by the geometry of the reed in order that this mechanism may excite the reed vibration. First, the flow

must separate from the reed at a sharp edge, so that the flow is attached on one side of the reed and separated on the other. A second requirement is that the side of fluid attachment must be that side of the reed which is away from the gaps. For example, if the equilibrium position of the reed were below the shallot, the vibration would not be excited by the flow. For this configuration the flow would decrease as the reed moved up, and the deceleration of the fluid would result in a high pressure on the upper surface of the reed. As a consequence, the energy of the reed vibration would be reduced. It is interesting to note that in

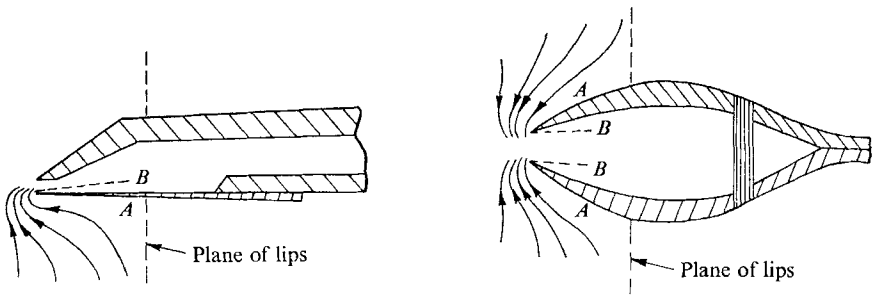

Clarinet reed Oboe reed

FIGURE 10. Sketches showing typical single and double reeds used in certain woodwind instruments: *A* denotes the side of the reed with attached flow, *B* denotes the side of the reed with separated flow.

the harmonica there is a reed on both the top and bottom walls of each of the small pressure chambers which are supplied with air by the mouth. There is a flow past both reeds during both the blowing and sucking modes of operation, but only one of the two reeds is excited by each mode. The reed which lies inside the chamber is excited by blowing whereas the one which lies on the outside of the opposite wall is excited by sucking.

It is thought that the mechanism which is described in this paper could also excite the vibrations of other types of reeds. Sketches of single and double reeds, as used in the clarinet and oboe respectively, are shown in figure 10. It can be seen that these reeds satisfy the requirements on the geometry with respect to a gap of varying size and a sharp edge at which the flow can separate. In addition, the condition that the flow be attached to the side of the reed away from the gap is also satisfied by these reeds.

The authors wish to thank Professor T. S. Lundgren for suggestions concerned with the potential flow model. One of the authors (A. O. St H.) acknowledges the support received under a National Science Foundation Traineeship. The paper is based in part on the Ph.D. dissertation submitted by one of the authors (A. O. St H.) to the faculty of the University of Minnesota.

REFERENCES

ANDERSON, A. B. C. 1955 Structure and velocity of the periodic vortex-ring flow pattern of a primary Pfeifenton (pipe tone) jet. *J. Acoust. Soc. Am.* **27**, 1048–1053.

BEAVERS, G. S. & WILSON, T. A. 1970 Vortex growth in jets. *J. Fluid Mech.* **44**, 97–112.

BIRKHOFF, G. & ZARANTONELLO, E. 1957 *Jets, Wakes, and Cavities.* Academic.

BROWN, G. B. 1937 The vortex motion causing edge tones. *Proc. Phys. Soc.* **49**, 493–507.

CHANAUD, R. C. & POWELL, A. 1965 Some experiments concerning the hole and ring tone. *J. Acoust. Soc. Am.* **37**, 902–911.

COLTMAN, J. W. 1968 Sounding mechanism of the flute and organ pipe. *J. Acoust. Soc. Am.* **44**, 983–992.

CREMER, VON L. & ISING, H. 1967 Die selbsterregten Schwingungen von Orgelpfeifen. *Acustica*, **19**, 143–153.

CURLE, N. 1953 The mechanics of edge tones. *Proc. Roy. Soc.* A **216**, 412–424.

WILSON, T. A., BEAVERS, G. S., DECOSTER, M. A., HOLGER, D. K. & REGENFUSS, M. D. 1971 Experiments on the fluid mechanics of whistling. *J. Acoust. Soc. Am.* (in Press).

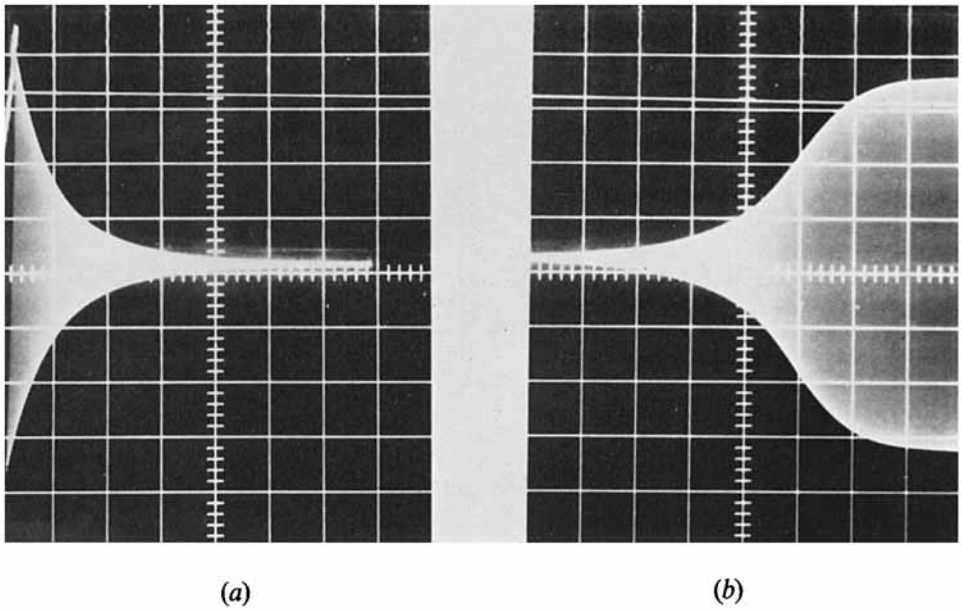

FIGURE 2. Typical oscillograms showing (*a*) the decay, and (*b*) the growth of the vibration amplitude: (*a*) flow rate too low to excite vibrations; (*b*) flow rate high enough to promote reed excitation.

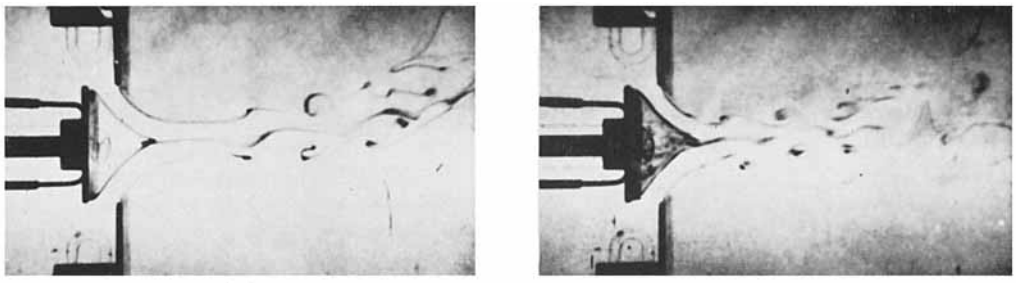

FIGURE 5. Photographs showing vortex pattern downstream of a stationary reed for $h/a = 4{\cdot}37$: (*a*) low flow rate; (*b*) high flow rate.

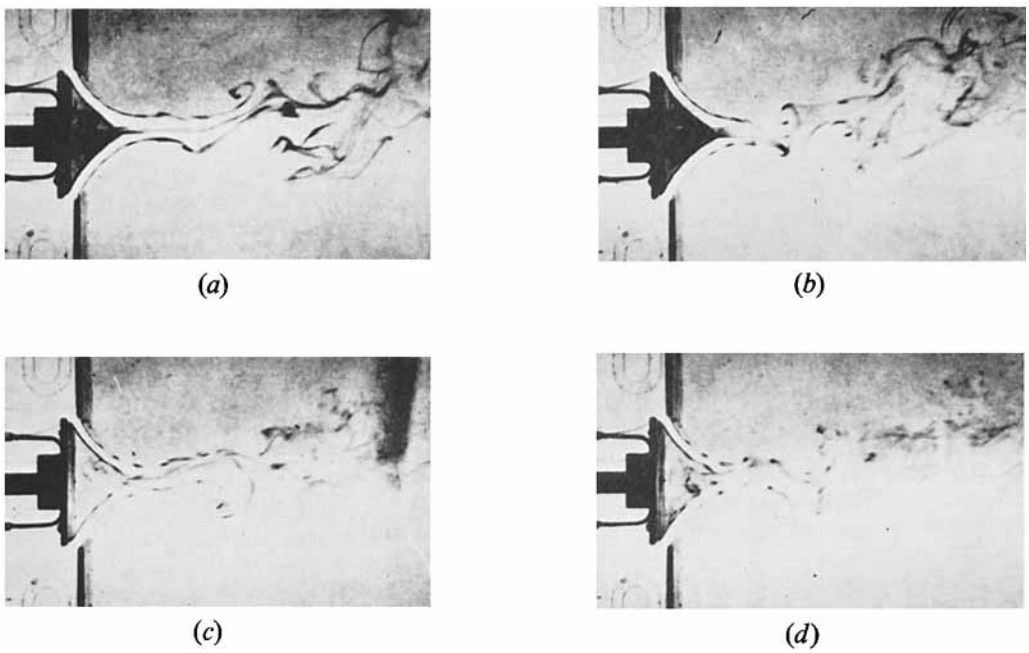

FIGURE 6. Comparison of the flow patterns for stationary and oscillating reeds: (*a*) and (*b*) are at identical flows; (*c*) and (*d*) are at identical flows.